Applied Catalysis A: General 391 (2011) 110–117

Contents lists available at ScienceDirect

Applied Catalysis A: General

journal homepage: www.elsevier.com/locate/apcata

Effect of Fe, Ga, Ti and Nb substitution in ≈$SbVO_4$ for propane ammoxidation

Andreas Wickman, Arne Andersson*

Department of Chemical Engineering, Lund University, Chemical Center, P.O. Box 124, SE-221 00 Lund, Sweden

ARTICLE INFO

Article history:
Received 4 January 2010
Received in revised form 2 April 2010
Accepted 21 April 2010
Available online 29 April 2010

Keywords:
Propane ammoxidation
Acrylonitrile
Sb-V-oxide based catalysts
≈$SbVO_4$
Substitutions with Fe
Ga
Ti and Nb
XRD
DRIFT
Raman spectroscopy

ABSTRACT

Substitution in rutile-type ≈$SbVO_4$ was made with Fe^{3+} and Ga^{3+} replacing V^{3+}, and Nb^{5+} replacing Sb^{5+}. Moreover, preparations with Ti were synthesised where Ti^{4+} ions substitute for both V^{4+} and V^{3+}/Sb^{5+} pairs. ≈$SbVO_4$-related phases containing Ti together with Fe and Ga were also prepared. The samples were characterised using X-ray diffraction, DRIFT and Raman spectroscopy. The characterisations show the formation of a cation deficient single rutile-type phase. Use of the samples in propane ammoxidation to produce acrylonitrile reveals, compared with the pure ≈$SbVO_4$ phase, that Fe, Ga and Ti substitution in ≈$SbVO_4$ results in lower activity but considerably higher selectivity to acrylonitrile at the same level of propane conversion. Niobium substitution, on the contrary, gives no improved catalytic properties. Correlations are presented between the catalytic and structural properties of the catalysts. It is demonstrated that isolation in the structure of the propane activating V–O· sites in a surrounding of nitrogen inserting Sb-sites results in improved selectivity for acrylonitrile formation.

1. Introduction

Currently there is a great interest in developing heterogeneous catalysts for producing useful chemicals from alkanes [1,2]. Regarding the production of acrylonitrile, presently it is produced by ammoxidation of propene over either promoted iron antimonates or multicomponent bismuth molybdate catalysts [2,3]. In recent years the interest in developing a heterogeneous catalyst for the one-step ammoxidation process of propane for production of acrylonitrile has become increasingly larger. The benefits of such a process are that propane is substantially cheaper than propene and far more abundant, rendering a lower production cost of acrylonitrile [3,4]. The best catalyst system discovered so far for propane ammoxidation is the MoV(Nb,Ta)(Te,Sb)O system, for which the primary patents are reporting yields up to 62% of acrylonitrile [5,6]. The second best system, with yields up to 40%, is the modified Sb-V-O system [7–9], where the rutile-type ≈$SbVO_4$ phase is an important catalyst component [7].

The pure ≈$SbVO_4$ is cation-deficient [10] and has been shown in previous investigations to not be active and selective for acrylonitrile formation [11,12]. However, the presence of excess antimony oxide (Sb:V > 1) in the catalyst results in improved performance [7–9,11–15]. According to patents [7,16–19], incorporation of Al, W, Sn, Ti, Fe and Ga to the catalyst composition likewise give enhanced catalytic properties. In the literature substitution of V by small amounts of Fe has been reported to increase the activity and decrease the selectivity to acrylonitrile, whereas larger amounts have the opposite effect [20]. Other additions that have been attempted include Cr [21,22] and Mo [23]. Also Nb has been reported to have some positive effect on both the activity and the selectivity when present in the V-Sb-Nb [15], Cr-V-Sb-Nb- [24] and Sn-V-Sb-Nb- [25,26] mixed oxide systems. Moreover, both alumina and niobia have been investigated as supports for Sb-V-oxide [27–29], showing below nonolayer coverage that the niobia supported material is more active and selective compared to that on alumina [27]. On the contrary, for a load above one monolayer, the alumina supported material is the best performing [27]. However, the results reported in the literature about the effect of substitutions are not always conclusive considering that the activities rarely are expressed per unit surface area. Moreover, the selectivity data compared are not always for the same temperature and degree of propane conversion.

Our previous investigations of the Sb-V-O [12], Al-Sb-V-O [30], Al-Sb-V-W-O [9] and Sb-V-Ti-O [31] systems have demonstrated that the improved catalytic properties of these systems compared with the pure ≈$SbVO_4$ phase are in accordance with the site isolation theory. The theory, which was originally developed by Callahan and Grasselli [32,33], states that the selectivity of a catalyst is dependent on the creation of structural isolation of the active site and limitation of the number of active oxygen species.

* Corresponding author. Tel.: +46 46 222 82 80; fax: +46 46 14 91 56.
E-mail address: Arne.Andersson@chemeng.lth.se (A. Andersson).

0926-860X/$ – see front matter © 2010 Elsevier B.V. All rights reserved.
doi:10.1016/j.apcata.2010.04.041

Thus, enhancement of the acrylonitrile selectivity in the rutile-type ≈$SbVO_4$ system can be achieved through substitution of some of the vanadium or antimony atoms in the crystal structure.

The oxidised form of ≈$SbVO_4$ has been reported to have the approximate composition $Sb_{0.92}{}^{5+}V_{0.28}{}^{3+}V_{0.64}{}^{4+}\square_{0.16}O_4$ where □ denotes cation vacancies [10,34,35]. Considering the valences of the cations, other metals can replace the vanadium and the antimony if they have the same valence and are of similar size. The ionic radii of V^{3+}, V^{4+} and Sb^{5+} are 0.64, 0.58 and 0.60 Å, respectively, and for Fe^{3+}, Ga^{3+}, Ti^{4+} and Nb^{5+} these are 0.64, 0.62, 0.61 and 0.64 Å, respectively [36]. Thus, it is of interest to try the substitution of V and Sb with Fe, Ga, Ti and Nb in the rutile-type ≈$SbVO_4$. In the present investigation such attempts are made to achieve isolation and dispersion of the active sites on the catalyst surface. Particularly the degree of isolation and dispersion of the active site is investigated regarding activity and selectivity for the ammoxidation of propane to give acrylonitrile.

2. Experimental

2.1. Catalyst preparation

The catalysts were made from powders of Sb_2O_3 (≥99%), V_2O_5 (99.5%), TiO_2 (≥99%), NbO_2 (>99%), $Ga(NO_3)_3$ (99.9%), and $Fe(NO_3)_3$ (≥99%).

Pure ≈$SbVO_4$ was prepared by the addition of 15.4 g V_2O_5 to a mixture of 515 ml water and 80 g of 30 wt.% hydrogen peroxide in water to form peroxovanadium ions [17,37]. After 20 min of stirring, 24.6 g Sb_2O_3 powder was added, and the resulting mixture was stirred for 3 h while heating in a covered beaker. To reduce the water volume through evaporation, the mixture was then heated in an uncovered beaker. When the mixture could no longer be stirred it was placed in an oven and dried at 120 °C for 16 h. Thereafter, the mixture was calcined in air at 650 °C for 16 h followed by a short calcination at 750 °C for 2 h. The material was then crushed and sieved to give particles with diameters in the range of 150–425 μm.

Catalysts with Fe, Ga, Ti and Nb replacing some V and Sb in ≈$SbVO_4$ were prepared using the same procedure as being described above to produce the pure ≈$SbVO_4$ catalyst. The appropriate amounts of the substitutes were added immediately before the volume of the mixture was reduced through evaporation. Substitutions with either of Fe, Ga or Ti were prepared with the nominal composition $Sb_{0.9}V_{0.9-x}M_xO_y$ where M being Fe, Ga or Ti, y being determined by the valences of the cations, and x being 0.2 (Fe, Ga and Ti) and in one case 0.4 (Ti). Substitutions with Ti and either Fe or Ga were made with the nominal composition $Sb_{0.9}V_{0.9-x-z}Ti_xM_zO_y$ where $x = 0.2$, M being Fe or Ga, z being 0.2, and y being determined by the valences of the cations. Moreover, a sample with Ti, Fe and Ga was prepared having the nominal composition $Sb_{0.9}V_{0.9-x-2z}Ti_xFe_zGa_zO_y$ with $x = 0.2$, $z = 0.1$, and y being determined by the valences of the cations. Regarding the niobium substitution, three samples were prepared with the nominal composition $Sb_{0.9-x}V_{0.9}Nb_xO_y$ where y is determined by the valences of the cations, and x being 0.009, 0.045 and 0.18, corresponding to 1, 5, and 20% replacement, respectively, of the antimony content in ≈$SbVO_4$.

The prepared catalysts are denoted according to Table 1. Since the calcination conditions varied between the samples to obtain substitution, the temperature and the duration of the final calcination in air are included in Table 1.

2.2. Catalyst characterisation

Specific surface areas were measured with a Micromeritics Flowsorb 2300 instrument using the BET-method with adsorption of nitrogen at the liquid nitrogen temperature. The catalyst samples were degassed at 350 °C. The specific surface areas of the samples are given in Table 1.

X-ray diffraction (XRD) patterns were recorded on a Seifert XRD 3000 TT diffractometer using Ni-filtered Cu Kα radiation and Si as an internal standard. The measurements were made on ground samples in a rotating sample holder.

Diffuse reflectance infrared Fourier transform (DRIFT) spectra were recorded on a Mattson Polaris spectrometer equipped with a liquid nitrogen-cooled broad band MCT-detector and a Harrick Scientific Praying Mantis diffuse reflection attachment. Spectra were recorded in dry air, and the samples were diluted to 1 wt.% of sample with KBr. A resolution of 4 cm^{-1} was used and for each sample 1000 scans were collected.

Fourier transform Raman (FT-Raman) spectra were collected using a Bruker IFS 66 FTIR spectrometer equipped with a Bruker FRA 106 FT-Raman device, a Nd:YAG laser and a germanium diode detector. The measurements were performed under ambient conditions on uncrushed catalyst particles in 5-mm quartz tubes. The laser power was set at 50 mW, the resolution was 4 cm^{-1}, and 1000 scans were recorded for each sample at 180° backscattering.

2.3. Activity measurements

The activity measurements were performed using a plug-flow reactor made from quartz glass, operating at atmospheric pressure. The inner diameter of the reactor was 6 mm, and the length was 600 mm. Moreover, the catalyst samples were diluted with quartz to maintain isothermal conditions in the reactor where the temperature was held at 480 °C. The ratio of the reactants in the inlet flow corresponded to the stoichiometric ratio of propane, ammonia and oxygen for acrylonitrile formation (propane:ammonia:oxygen:water vapour:nitrogen = 1:1:2:0.5:2.5). Water vapour was added to the inlet flow to assist in the control of the reaction temperature of the exothermic reaction. A total inlet flow of 70 ml STP/min was passed through the catalyst bed. The conversion was varied by varying the amount of catalyst being subjected to the flow, usually in the range 0.1–4.8 g (WHSV = 42,000–875 ml/h g) depending on the activity of the sample. Propane, propylene, acrylonitrile, acetonitrile and carbon oxides were analysed using an on-line gas chromatograph equipped with a Porapak Q column, an FID detector, and a methanation column making possible the analysis of carbon oxides in the form of methane. Of the degradation products formed, the largest part was carbon oxides. The selectivity to acetonitrile was lower, usually of the order 5%. Experiments varying the total flow rate and the catalyst particle size at fixed residence time confirmed that the activity measurements are affected by neither external nor internal mass transfer limitations.

The catalytic data presented are for steady-state conditions, which for the samples listed in Table 1 were reached almost immediately. After the first 20 min no changes of conversion and selectivity were observed during the measurements, which continued for 4 h.

3. Results

3.1. Specific surface area

The specific surface areas of the prepared samples are displayed in Table 1. The surface area of the pure rutile ≈$SbVO_4$ is about 2 m^2/g. Substitution with titanium does not affect the surface area very much (~3 m^2/g). However, incorporation of gallium and iron produce samples with surface areas of the order 10 m^2/g. The low values of the specific surface areas of the niobium containing sam-

Table 1
Notation, nominal composition, calcination conditions and specific surface area of the prepared catalysts.

Catalyst notation	Metal atom ratio	Calcination in air	Specific surface area (m^2/g)
SV (≈$SbVO_4$)	Sb:V = 1:1	650 °C, 16 h + 750 °C, 2 h	1.7
SVT-972	Sb:V:Ti = 9:7:2	650 °C, 28 h	3.1
SVT-954	Sb:V:Ti = 9:5:4	650 °C, 28 h	3.6
SVF-972	Sb:V:Fe = 9:7:2	650 °C, 16 h	11.9
SVG-972	Sb:V:Ga = 9:7:2	650 °C, 16 h	11.1
SVTF	Sb:V:Ti:Fe = 9:5:2:2	650 °C, 24 h	12.0
SVTG	Sb:V:Ti:Ga = 9:5:2:2	650 °C, 24 h	9.8
SVTFG	Sb:V:Ti:Fe:Ga = 9:5:2:1:1	650 °C, 24 h	9.8
SVN1	Sb:V:Nb = 8.91:9.00:0.09	650 °C, 32 h + 750 °C, 16 h	0.5
SVN5	Sb:V:Nb = 8.55:9.00:0.45	650 °C, 32 h + 750 °C, 8 h	0.5
SVN20	Sb:V:Nb = 7.2:9.0:1.8	650 °C, 32 h + 750 °C, 8 h	1.9

ples can be explained by the more severe calcination conditions being required in this case to obtain the desired rutile phase.

3.2. X-ray diffraction

Fig. 1 shows the XRD patterns for ≈$SbVO_4$ (SV) and the substitutions with Ti, Fe and Ga. The diffractogram of the SV sample displays lines only from the rutile-type oxidised ≈$SbVO_4$ phase [13,34,35,38]. Reflections from a related rutile-type phase are present in the diffractograms of the samples with Ti, Fe and Ga. The samples with two and three substituting elements (SVTF, SVTG and SVTFG), moreover, present some lines from α-Sb_2O_4 [39].

In Fig. 2 are the X-ray diffractograms for the Sb-V-Nb-O samples compared with that for ≈$SbVO_4$. It is seen that all samples with niobium show reflections from an ≈$SbVO_4$-related rutile-type phase. The SVN1 and SVN5 samples, besides the lines from the rutile, display a weak line at $\Theta = 15.4^\circ$, which cannot be assigned as no companion peaks appear. In the XRD of SVN20 there are peaks at 12.2, 14.8, 18.5, 22.3, and 24.8° Θ, which are not from a rutile-type phase. However, a comparison with the data in the JCPDS file [39] shows that the lines do not fit to any data being reported for an oxide with one or more of the elements Sb, V and Nb. Also, no fit was obtained using the JCPDS search library.

X-ray analyses of the samples after use in propane ammoxidation revealed no significant difference compared to the freshly prepared samples and show no change in either phase composition or particle size. The fact that the rutile samples are stable in ammoxidation agrees with previous in situ characterization, where it was observed for alumina supported samples that dispersed V and Sb species react during propane ammoxidation to form rutile type ≈$SbVO_4$ [40,41].

3.3. Diffuse reflectance FTIR spectroscopy

DRIFT spectra of the region below 1200 cm^{-1} from prepared samples are shown in Fig. 3. Bands in this region provide information about the metal–oxygen vibration modes. All the sample spectra in Fig. 3 are characterised by a prominent peak at 1015 cm^{-1}

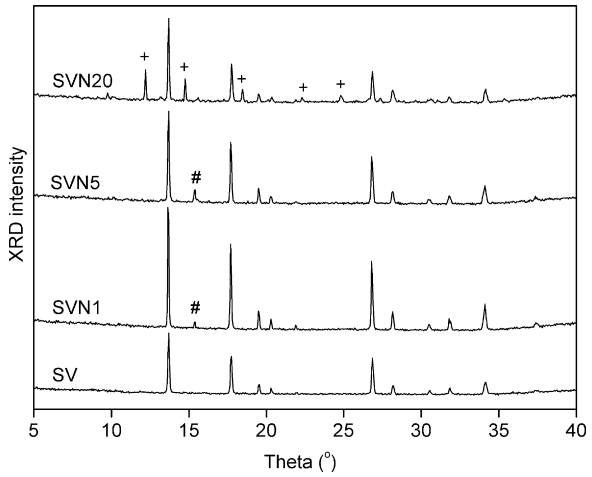

Fig. 2. XRD patterns for ≈$SbVO_4$ (SV) and its substitutions with Nb (notations as in Table 1). The diffractograms of SVN1 and SVN5 show an unidentified peak (#) and that of SVN20 shows several reflections (+) which are possibly from a niobium oxide.

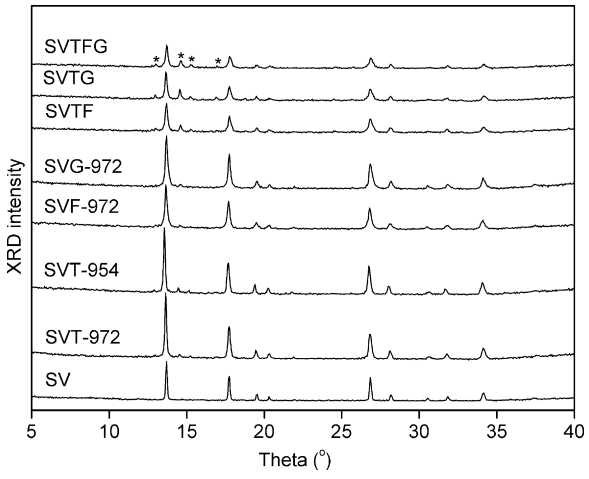

Fig. 1. XRD patterns of ≈$SbVO_4$ (SV) and substitutions with Ti, Fe and Ga (notions as in Table 1). The positions of the four strongest reflections from α-Sb_2O_4 are marked with an asterisk.

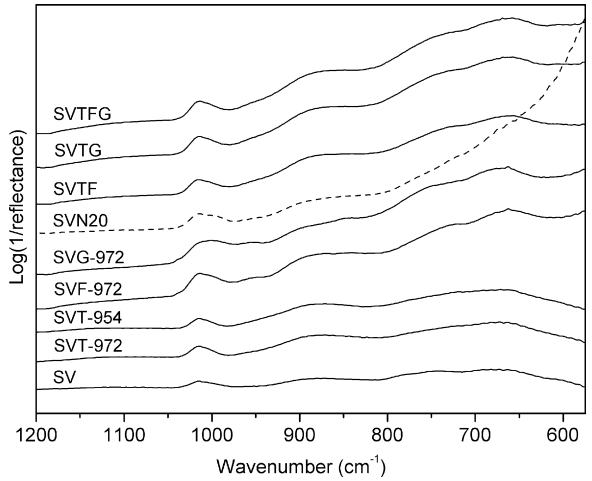

Fig. 3. DRIFT spectra of ≈$SbVO_4$ (SV) and the corresponding preparations with Ti, Fe, Ga and Nb.

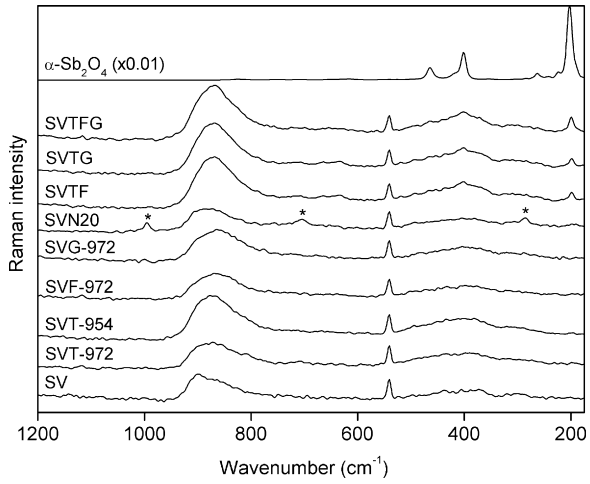

Fig. 4. Raman spectra of α-Sb_2O_4, ≈$SbVO_4$ (SV) and the samples with Ti, Fe, Ga, and Nb. In the spectrum for SVN20 are bands from V_2O_5 marked with an asterisk. The peak at 540 cm^{-1} is an instrumental artefact peak that can be used for quantitative comparisons.

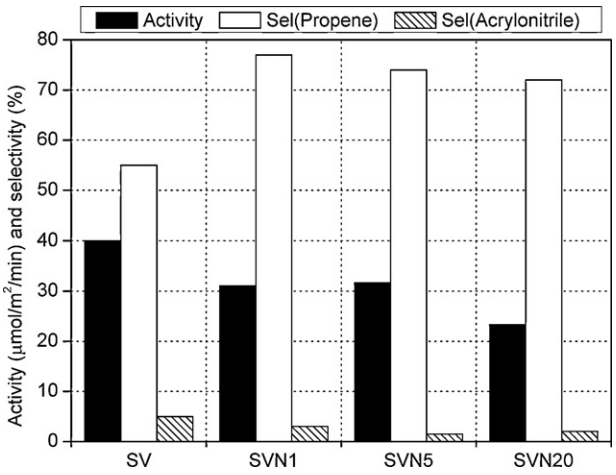

Fig. 5. Propane ammoxidation over ≈$SbVO_4$ (SV) and the Sb-Nb-V-O catalysts. Initial reaction rate per unit surface area of the catalyst (activity) and selectivity to propene and acrylonitrile at 5% propane conversion. Reaction conditions: 480 °C with the feed propane:ammonia:oxygen:steam:nitrogen = 1:1:2:0.5:2.5.

and a broad band at 880 cm^{-1}. These bands are typical for the rutile-type ≈$SbVO_4$ structure with cation vacancies [10]. Additionally, the DRIFT spectra of SV and the samples with Ti, Fe and Ga show a broad band at 670 cm^{-1} with a shoulder band at about 730 cm^{-1}, which are typical rutile bands [42,43]. The latter bands were present in the spectra for SVN1 and SVN5 while SVN20, as shown in Fig. 3, presents strong absorption in the region below 800 cm^{-1}.

3.4. Raman spectroscopy

The FT-Raman spectra of a selection of prepared catalysts are shown in Fig. 4 together with a spectrum of α-Sb_2O_4. The catalyst samples are poor Raman scatterers and show, compared with α-Sb_2O_4, only peaks with low intensities. In the spectrum of ≈$SbVO_4$ there is a relatively broad peak at 880 cm^{-1} and a very weak and broad band around 400 cm^{-1}, which both are characteristic of the cation-deficient ≈$SbVO_4$ [11,44]. As Fig. 4 shows, the same two bands are present in the spectra of all catalysts. Besides the ≈$SbVO_4$ rutile-type related bands, the SVN20 sample displays peaks at 994, 701 and 284 cm^{-1}, which can be assigned to V_2O_5 [11,45]. Further, no bands from V_2O_5 were present in the spectra of SVN1 and SVN5 with lower niobium content (not shown). Considering Fig. 4, α-Sb_2O_4 displays strong Raman bands at 463, 402 and 201 cm^{-1} [9,46] and the two strongest bands of these appear in the spectra of SVTF, SVTG and SVTFG.

3.5. Activity measurements

Fig. 5 presents a comparison of ≈$SbVO_4$ (SV) and the analogues with Nb. The Nb-samples show lower activity and there is a trend that the activity decreases with increased Nb-content. At 5% propane conversion the Nb-samples, compared with ≈$SbVO_4$, are more selective to the formation of propene and less selective to acrylonitrile. Due to SVN1 and SVN2 have lower surface areas than SVN20 (Table 1) the latter sample was selected for further investigation and comparison with the samples containing Ti, Fe and Ga.

Fig. 6 shows data for SV, SVN20 and the substitutions with one of Ti, Fe and Ga. The figure compares the catalysts regarding the activity and the highest selectivity to acrylonitrile obtained by varying the amount of sample. The corresponding data for the selectivity to propene as well as the propane conversion are included in the figure. Considering the selectivity and conversion data for SVN20, it is obvious that this catalyst gives no improvement compared to SV. The highest selectivity to acrylonitrile over SVN20 is 13% and is obtained at 10% propane conversion, corresponding to a yield of 1.3%. For SV the best selectivity is 12% at 13% propane conversion, giving a yield of 1.6% of acrylonitrile. In comparison to SV, the catalysts with titanium SVT-972 and SVT-954 show lower activity. With increase of the Ti-content the activity is decreased and the selectivity to acrylonitrile is increased. Over SVT-954 the selectivity to acrylonitrile reaches 44% at 25% propane conversion, which is equal to a yield of 11% per single pass. The catalysts with Fe (SVF-972) and Ga (SVG-972) are considerably less active than ≈$SbVO_4$ (SV) and the analogues with Ti and Nb. However, compared with SV, the former samples are more selective to acrylonitrile and the selectivity maximum is obtained at higher propane conversion. Also, compared with SVT-972, the same nominal substitution level of Ga (SVG-972) and, especially, Fe (SVF-972) renders a higher selectivity to acrylonitrile at a higher conversion level. The highest selectivity obtained for acrylonitrile formation over SVT-972, SVG-972 and SVF-972 is 16, 18 and 28%, respectively. For SVT-972 and SVF-972 the corresponding selectivity to propene is about 32% and somewhat lower for SVG-972.

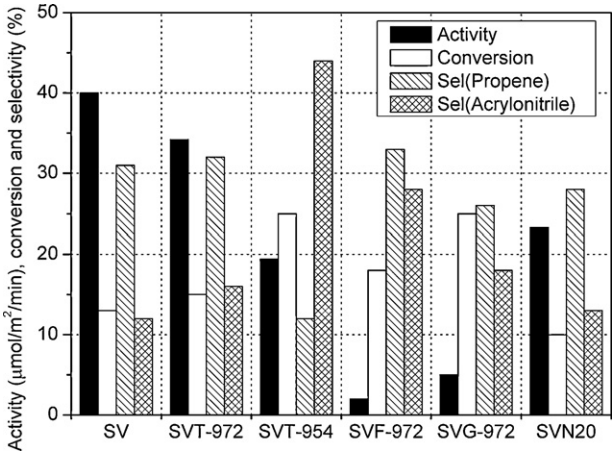

Fig. 6. Propane ammoxidation over ≈$SbVO_4$ (SV) and the substitutions with one of Ti, Fe, Ga and Nb. Besides the activity, the figure gives the highest selectivity to acrylonitrile that is obtained varying the amount of catalyst, the corresponding data for the selectivity to propene and the propane conversion. Reaction conditions: 480 °C with the feed propane:ammonia:oxygen:steam:nitrogen = 1:1:2:0.5:2.5.

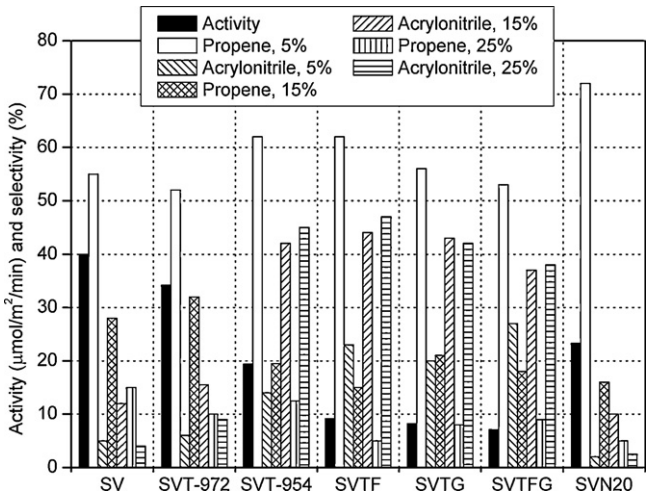

Fig. 7. Propane ammoxidation over a selection of catalyst compositions (see Table 1). Initial reaction rate per unit surface area of the catalyst (activity) and selectivity to propene and acrylonitrile formation at 5, 15, and 25% propane conversion. Reaction conditions: 480 °C with the feed propane:ammonia:oxygen:steam:nitrogen = 1:1:2:0.5:2.5.

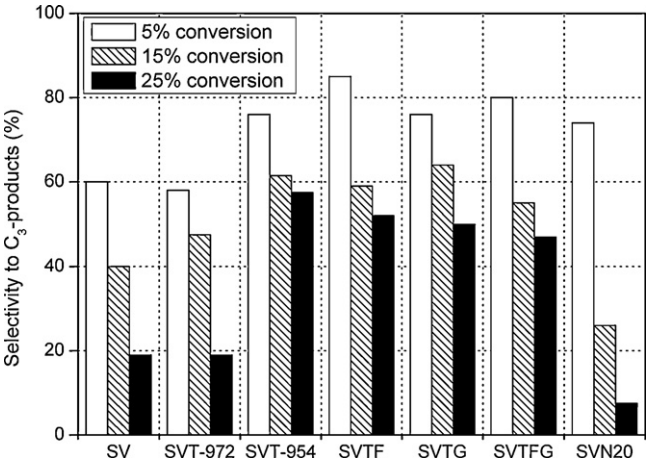

Fig. 8. Propane ammoxidation over a selection of catalyst compositions (see Fig. 7). Total selectivity to the formation of C_3-products (propene and acrylonitrile) at 5, 15, and 25% propane conversion. Reaction conditions: 480 °C with the feed propane:ammonia:oxygen:steam:nitrogen = 1:1:2:0.5:2.5.

Previous investigations [31,47] have shown that there is great improvement of the performance of the catalyst when the vanadium in ≈$SbVO_4$ is diluted and isolated in the structure through the partial replacement with Ti (compare SVT-972 and SVT-954 in Fig. 6). Considering the results in Fig. 6, it was considered to be of interest combining Ti with Fe and Ga as replacement for some of the vanadium in ≈$SbVO_4$. The composition of SVT-972 was selected as a base for the further replacement of vanadium with Fe and Ga up to the substitution level corresponding to that for SVT-954. The samples are denoted SVTF, SVTG and SVTFG, and the nominal compositions of the samples are given in Table 1. Thus, of special interest is to compare the catalytic performances of the latter samples with the performances of SVT-972 and SVT-954. Figs. 7 and 8 give such a comparison of the samples for 5, 15 and 25% propane conversion and include as well data for SV and SVN20. The levels of conversion were chosen to highlight the initial product distribution as well as showing the ability of the samples to convert the formed propene to the desired product acrylonitrile. The latter point is important, considering that previous investigations have shown that propene is the major intermediate in acrylonitrile formation from propane [11,48].

Fig. 7 shows, compared with SVT-972, that further replacement of V with Fe and Ga gives samples (SVTF, SVTG and SVTFG) which are less active but more selective to acrylonitrile formation at the same conversion level. Moreover, considering the total selectivity to the C_3-products propene and acrylonitrile, which is displayed in Fig. 8 for various conversion levels, it is apparent that SVTF, SVTG and SVTFG give higher selectivity to the C_3-products than is obtained over SV and SVT-972. This is especially the case at 25% of propane conversion, where the total selectivity is around 50% for the former samples to be compared with about 20% for SV and SVT-972. The data in Fig. 7 show that at 5% propane conversion the selectivity to propene and acrylonitrile is 52% and 6%, respectively, for SVT-972. With increase of the conversion the selectivity to acrylonitrile passes through a maximum and then decreases to 9% at 25% propane conversion, where the selectivity to propene is 10%. For SVTF and SVTG the selectivity to propene is of the order 60% at 5% propane conversion, and the corresponding selectivity to acrylonitrile is about 20%. When the conversion is increased, the selectivity to propene decreases and the selectivity to acrylonitrile increases. At 25% propane conversion, the selectivity to acrylonitrile and propene is around 45 and 7%, respectively, for both SVTF and SVTG. The SVTFG and SVT-954 samples show similar behaviour as SVTF and SVTG with increase of the conversion of propane (Figs. 7 and 8). For SVTFG, however, the selectivity data for acrylonitrile and propene are generally somewhat lower.

Incorporation of niobium into the ≈$SbVO_4$ structure does not give improved catalytic properties as confirmed by the data in Figs. 7 and 8. Compared with the non-substituted sample SV (≈$SbVO_4$), the SVN20 sample shows lower activity and selectivity to acrylonitrile and propene, except at the lowest conversion level.

Of the samples considered in Figs. 7 and 8, SVT-954 and SVTF have the best catalytic properties for propane ammoxidation. To better compare the samples, Fig. 9a shows the selectivity to propene as a function of the conversion of propane and in Fig. 9b are the corresponding plots of the selectivity and the yield to acrylonitrile. Data from a previous investigation [13] for a catalyst denoted SVWA with Sb:V:W:Al = 5:1:1:21 are also included in Fig. 9 because this composition is one of the best known so far for propylene ammoxidation among the modified ≈$SbVO_4$ rutile-type catalysts [7,9]. Fig. 9 shows similar values and variation with the propane conversion of the plots for SVT-954 and SVTF. The selectivity to propene formation decreases with increase of conversion, and the selectivity to acrylonitrile pass through a maximum of about 45% at 25% propane conversion. The maximum corresponds to a yield of about 11–12%. However, compared with the data for SVWA, this value is low. As Fig. 9 shows, for SVWA there is a selectivity maximum of 49% at 55% propane conversion, corresponding to a yield of 27%. Moreover, the selectivity to acrylonitrile decreases only slowly when the conversion of propane is further increased. The selectivity decreases to 47% at 81% propane conversion, which corresponds to a yield of 38% acrylonitrile.

4. Discussion

4.1. Substitution in ≈$SbVO_4$

The XRD pattern in Fig. 1 of the SV sample shows reflections only from the oxidised ≈$SbVO_4$ rutile-type phase $Sb_{0.92}V_{0.92}O_4$ [10,34,35,38]. The diffractograms in Fig. 1 of the samples with either of Ti, Fe or Ga replacing some of the vanadium (SVT-972, SVT-954, SVF-972 and SVG-972), likewise, show reflections belonging to the rutile-type structure. SVTF, SVTG and SVTFG with two or more substituents additionally show some distinct peaks from α-Sb_2O_4 [39].

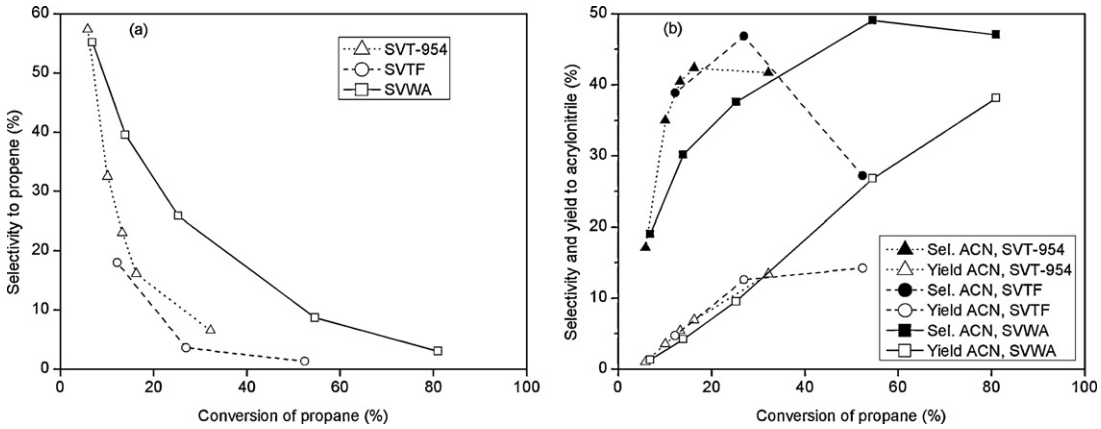

Fig. 9. A comparison of the ammoxidation of propane over SVT-954 (Sb:V:Ti = 9:5:4), SVTF (Sb:V:Ti:Fe = 9:5:2:2) and SVWA (Sb:V:W:Al = 5:1:1:21). (a) The selectivity to propene as a function of the conversion of propane and (b) the corresponding selectivity and yield to acrylonitrile. Reaction conditions: 480 °C with the feed propane:ammonia:oxygen:steam:nitrogen = 1:1:2:0.5:2.5. The catalytic data are for steady-state conditions. Opposed to the other samples, the SVWA sample showed a long activation period, lasting for about 15 h before reaching steady-state (see refs. [9,13]).

The presence of α-Sb_2O_4 in those samples is confirmed by the corresponding Raman spectra in Fig. 4, showing bands from the latter phase at 402 and 201 cm^{-1} [9,46]. Concerning the samples with Nb, the XRD patterns in Fig. 2 of SVN1 and SVN5, except for a weak unidentified peak, display only reflections from the rutile-type structure. When the content of niobium is increased, besides the lines from the rutile, several other peaks appear. Thus, the diffractograms in Fig. 2 indicate that the substitution limit of Sb for Nb is in the range 5–20 at.%. The non-rutile peaks in the XRD of SVN20 could not be identified considering the JCPDS files [39] but are possibly from a niobium oxide. In this case incomplete synthesis is confirmed by the Raman spectrum of SVN20 in Fig. 4, showing peaks from V_2O_5. In previous studies of V-Sb-oxide based multicomponent preparations containing Nb, formation of Nb_2O_5 [15,25,27], $SbNbO_4$ [15,27] and VNb_9O_{25} [24] have been observed. However, none of those phases can explain the unidentified XRD peaks in Fig. 2.

In the oxidised ≈$SbVO_4$ with the composition $Sb_{0.92}V_{0.92}O_4$ the cations are Sb^{5+}, V^{3+} and V^{4+} [10,34,38]. Substitution of V^{3+} (0.64 Å) with Fe^{3+} (0.64 Å) and Ga^{3+} (0.62 Å) are likely possible since the valences of the cations are the same and the ionic radii are almost identical. By the same reason, substitution of V^{4+} (0.58 Å) with Ti^{4+} (0.61 Å) and Sb^{5+} (0.60 Å) for Nb^{5+} (0.64 Å) should be possible. Except for SVN20 (Fig. 4), in no case any free vanadium, titanium, iron or gallium oxide were observed. The XRD patterns in Fig. 1 clearly show that Ti, Fe and Ga can replace vanadium in the ≈$SbVO_4$ structure and, moreover, the XRD data in Fig. 2 show that possibly Nb can replace some of the Sb. Substitution of V^{3+} with Fe^{3+} and Ga^{3+}, as well as Sb^{5+} with Nb^{5+} in ≈$SbVO_4$ is consistent with the existing rutile-type phases $FeSbO_4$ [49,50], $GaSbO_4$ [51,52] and $VNbO_4$ [53,54]. Moreover, it has been shown that substitution of V with Ti is possible in rutile type ≈$SbVO_4$ [31].

The preservation of the basic ≈$SbVO_4$ structure $Sb_{0.92}{}^{5+}V_{0.28}{}^{3+}V_{0.64}{}^{4+}\square_{0.16}O_4$ with cation vacancies □ [10,38] upon substitution of some V or Sb with Ti, Fe, Ga or Nb is shown by the DRIFT and Raman spectra in Figs. 3 and 4, respectively. The DRIFT spectra of the samples, besides the typical rutile bands below 800 cm^{-1} [42,43], show two unique bands at 1015 and 880 cm^{-1}. It has been demonstrated that the intensities of these bands relative to the intensities of the typical rutile bands below 800 cm^{-1} are proportional to the number of cation vacancies in the unit cell of the rutile-type phase [10], and the former bands can be assigned to metal–oxygen vibrations involving the two-coordinated oxygen species that are next to the cation vacancies [10,31]. Not less than 24% of the oxygen species in the oxidised ≈$SbVO_4$ are two-coordinated [47], while the remaining oxygens are three-coordinated as in the stoichiometric rutile structure [55]. Besides the two characteristic infrared bands at 1015 and 880 cm^{-1} (Fig. 3), the catalysts give a Raman band at 880 cm^{-1} (Fig. 4). The latter band is displayed by the oxidised and cation deficient ≈$SbVO_4$ phase and, likewise the two characteristic infrared bands, the Raman band disappears when the material is reduced forming stoichiometric $Sb_{0.9}V_{1.1}O_4$ without any cation vacancies [10,11,44].

Thus, from the discussion above, it follows that the prepared substitutions with Fe, Ga and Nb are cation vacant rutile-type phases with the approximate compositions $Sb_{0.9}{}^{+}V_{0.1}{}^{3+}M_{0.2}{}^{3+}V_{0.6}{}^{4+}O_4$ where M = V, Fe or Ga, and $Sb_{0.9-x}{}^{5+}Nb_x{}^{5+}V_{0.3}{}^{3+}V_{0.6}{}^{4+}O_4$ with $x < 0.18$ (SVN20). According to Millet and coworkers [20,56], Fe^{3+} in ≈$SbVO_4$ substitutes predominantly for V^{4+} forming a rutile-type structure with both cation and anion vacancies. However, as indicated above we rather believe that in our preparations the substitution mechanism $Fe^{3+} \leftrightarrow V^{3+}$ is more likely considering our previous study of the Al-Sb-V-oxide system [30]. In that work we present data clearly demonstrating that only a limited amount of the V in ≈$SbVO_4$ can be replaced by Al and that the substitution mechanism $Al^{3+} \leftrightarrow V^{3+}$ is obeyed. A possible reason for the differences observed concerning substitution with iron is that in the previous works [20,56] the calcination time was relatively short (3 h at 700 °C), whereas in the present case we have used a considerably longer calcination time (see Table 1) in order to obtain substitution.

Concerning substitution with Ti we have showed [31] that titanium substitutes for both V^{4+} and V^{3+}/Sb^{5+} pairs according to the two mechanisms $Ti^{4+} \leftrightarrow V^{4+}$ and $2Ti^{4+} \leftrightarrow V^{3+} + Sb^{5+}$. The fact that the latter mechanism occurs to some extent is in agreement with the XRD for SVT-954 in Fig. 1, showing small peaks from α-Sb_2O_4, peaks which also can be noticed as weak features in the XRD for SVT-972. For SVTF, SVTG and SVTFG with the with the same Sb/V ratio as SVT-954, the XRD peaks from α-Sb_2O_4 become even more intense as the XRDs in Fig. 1 show. Thus, it seems that the presence of trivalent Fe and Ga promotes the substitution mechanism with two Ti^{4+} substitute for one V^{3+} and one Sb^{5+}. Consequently, the composition of the samples with Ti can be formulated ≈$(Sb,Ti)_{0.9}(V,Ti,Fe,Ga)_{0.9}O_4$ with some α-Sb_2O_4.

4.2. Structure–activity/selectivity relationships

The catalytic data in Fig. 7 show that SVT-954, compared with SVT-972, is less active and more selective to acrylonitrile formation

at the same conversion level. Fig. 8, moreover, shows that the total selectivity to the C_3-products propene and acrylonitrile, especially at the higher conversion level of propane, is higher for SVT-954 than for SVT-972. The highest selectivity to acrylonitrile over the samples was 16% for SVT-972 and 44% for SVT-954 and was obtained at 15 and 25% propane conversion, respectively (see Fig. 6). This difference between the samples in catalytic performance has been reported being due to the samples having different content of V^{3+} ions and different Sb^{5+}/V^{3+} ratio [31,47]. As mentioned above, in our previous report on a $Sb_{0.9}V_{0.9-x}Ti_xO_4$ series with $0.1 < x < 0.9$ [31] it was demonstrated that the substitution of Ti occurs according to the two mechanisms $Ti^{4+} \leftrightarrow V^{4+}$ and $2Ti^{4+} \leftrightarrow V^{3+} + Sb^{5+}$. It was also shown for the series that there is a correlation between the activity and the content of V^{3+} in the unit cell, and that the selectivity to acrylonitrile could be correlated to the Sb^{5+}/V^{3+} ratio of the rutile-type phase. The correlations, of course, should be understood as correlations to the corresponding surface sites. The V^{4+} sites are possibly reoxidation sites, but the reoxidation step is not rate limiting [31]. The relationships reported suggest that the oxygen associated with V^{3+}, which has a partial radical character [3], is the propane activator and that Sb^{5+} is the nitrogen inserting element. Thus, an increase of the Sb^{5+}/V^{3+} ratio should increase the probability of nitrogen insertion and formation of acrylonitrile. These views agree with the rutile-related stoichimetric phase $Al_{1-x}{}^{3+}Sb^{5+}V_x{}^{3+}O_4$ ($0 < x < 0.5$) being active for propane ammoxidation and more selective than the pure $\approx SbVO_4$ [30]. Further support for the inference is given by a previous report on the oxydehydrogenation of propane over Mg-V-Sb-oxide [57], showing that the oxydehydrogenation of propane to form propene occurs on isolated V-sites and the oxidation of propene to acrolein involves Sb-sites.

Concerning the data in Fig. 5, these show that the substitution of Sb with Nb results in lower activity and suppression of acrylonitrile formation from the formed propene (lower acrylonitrile/propene ratio). The data in Figs. 6–8 for SVN20 at higher propane conversions confirm this trend, although with increase of the propane conversion there is an increased influence from the degradation of propene to form carbon oxides. The somewhat lower activity of the Nb-samples can obviously be explained by an influence from surrounding Nb atoms on the V-site activating propane. In light of the previous reports [31,47], compared with the SV sample ($\approx SbVO_4$), the lower initial selectivity of the Nb-samples towards acrylonitrile formation is due to the latter samples having lower Sb/V ratios. Thus, the results in Fig. 5 agree with Sb being the nitrogen inserting moiety and infer that Nb is unable to perform this step. Alternatively, Sb-NH-Sb centres are responsible for the nitrogen insertion step as in propene ammoxidation over Fe- and U-antimonate catalysts [58] and Nb/Sb pairs are unable to activate ammonia properly. As demonstrated, our data on Nb clearly can be rationalised considering previous knowledge. However, in other studies of propane ammoxidation on unsupported mixed oxide systems with V/Sb/Nb [15], Cr/V/Sb/Nb [24] and Sn/V/Sb/Nb [25,26] some positive effects of Nb addition have been observed on activity and selectivity, demonstrating the importance of the phase composition.

The data in Fig. 6 show that the activity is considerably lower for SVF-972 and SVG-972 than for SV and the samples with Ti and Nb. This fact is a direct evidence for the activation of propane involves V^{3+} sites and that Fe^{3+} and Ga^{3+} selectively replace V^{3+} in the $\approx SbVO_4$ structure, while Nb^{5+} and Ti^{4+} substitute for Sb^{5+} and V^{4+}/V^{3+}-Sb^{5+}, respectively. That Fe^{3+} sites have low activity for propane activation agrees with $FeSbO_4$ having low activity for propane ammoxidation [59,60]. Further, the results in Fig. 6 show that the selectivity to acrylonitrile is higher for SVF-972 than is obtainable over SV and SVT-972 with the same substitution level as SVF-972. This result is consistent with propene being an intermediate for acrylonitrile formation from propane [11,48] and that $FeSbO_4$ with Sb:Fe > 1 is a catalyst for propene ammoxidation [2,3] and partial oxidation [49,61–63]. Also, the SVG-972 sample is more selective to acrylonitrile compared to the SV sample, which agrees with rutile-type $GaSbO_4$ has been found active for propane ammoxidation to acrylonitrile [52]. However, the activity of $GaSbO_4$ is only of the order 0.4 μmol/m^2/min at 550 °C. This value is considerably below the values in Figs. 5–7 being measured at 480 °C for the present samples with vanadium, showing that vanadium is a cardinal element for the activation of propane but that Ga-sites possibly can activate propene. The higher selectivity of SVF-972 and SVG-972 for acrylonitrile formation compared with the corresponding values for SV, SVT-972 and SVN20, are consistent with the indication that the Sb^{5+}/V^{3+} ratio of the former samples being higher. Compared with SVF-972, higher substitution levels of Fe for V was required in a previous study to give similar results i.e. lower activity and higher selectivity compared to the unsubstituted $\approx SbVO_4$ [20,56]. The difference compared to our results is in line with the fact that a relatively longer calcination time has been used in the present investigation.

In Figs. 7 and 8 the performances of SVT-972 and SVT-954 are compared with those of SVTF, SVTG and SVTFG. The activity of SVT-954 is lower than that for SVT-972, showing that with increase of the amount of titanium substitution the activity decreases. However, the data for SVTF, SVTG and SVTFG show that the activity is decreased even more when the substitution includes Fe and Ga. This fact agrees with Fe and Ga selectively replacing the V^{3+} sites being responsible for the activation of propane, while Ti replaces both V^{4+} ions and V^{3+}/Sb^{5+} couples [31].

Although Ti, Fe and Ga have different property regarding the transformation of the propene intermediate, the data in Figs. 7–8 can be rationalised in terms of the site isolation concept proposed by Callahan and Grasselli [32,33]. A comparison of the catalytic data for the samples containing Ti, Fe and Ga with those for SV ($\approx SbVO_4$) demonstrates that isolation of the active vanadium sites in the catalyst structure, through replacement with other elements, results in improved selectivity to acrylonitrile formation. The similar conclusion has previously been drawn rationalising data for the ammoxidation of propane over the Sb-V-O system with Al [30], W [9] and Ti [31]. Besides the present results on Ti, Fe and Ga substitution, also Cr [21,22], Mo [23] and Nb [15,24–29] addition have been found to give some improvement compared to the unsubstituted $\approx SbVO_4$ base. However, among $\approx SbVO_4$ derived catalysts, those with Al and W incorporated in the rutile structure are presently the best being reported for propane ammoxidation so far [7,9,13]. Data for such a catalyst (SVWA), which has previously been characterised [9,13], are displayed in Fig. 9 and compared with data for the SVTF and SVT-954 samples. Compared with SVWA having the nominal composition Sb:V:W:Al = 5:1:1:21, the SVTF and SVT-954 samples give higher selectivity to acrylonitrile at low conversions (< 35%) but for SVWA the selectivity continues to increase up to 55% propane conversion. The high selectivity for the latter sample is then retained with the further increase of the propane conversion, and a yield of 38% acrylonitrile is obtained at 81% propane conversion. Opposed to the other samples, our previous characterization [9,13] of the SVWA sample showed a long activation period (~15 h) before steady-state is reached. During that period, under influence of the reaction W^{6+} becomes reduced, forming rutile type $\approx Sb_{0.9}V_{0.9-x}W_xO_4$ from an unselective and not very crystalline precursor. Thus, the results of the present investigation confirm that the activity and the selectivity of the catalyst can be tuned at the atomic level and, moreover, give new openings for further work on modification of the active ensemble of $\approx SbVO_4$.

The fact that our results clearly support that there is a relationship between activity and the phase content of V^{3+} and also between selectivity and the Sb^{5+}/V^{3+} ratio of the phase, indicates that the bulk features extend up to the surface. In support of this inference, besides the present results is the fact that the surface

composition as obtained by XPS for the pure $\approx SbVO_4$ without excess Sb is almost the same as that of the bulk and, moreover, is unchanged after the sample has been subjected to propane ammoxidation [44]. Also, unlike samples with excess Sb, the pure phase show stable catalytic performance with time and consists of well faceted crystals with clean surfaces [12]. Furthermore, it has been demonstrated that the rutile type structure is stable under ammoxidation conditions [40,41]. The latter fact, however, does not exclude that the steady-state composition of the rutile can be slightly reduced, preserving the rutile type structure as previously being reported with less number of cation vacancies [10].

5. Conclusions

In rutile type $Sb_{0.9}{}^{5+}V_{0.3}{}^{3+}V_{0.6}{}^{4+}O_4$ substitution of V with Fe, Ga and Ti is possible. The predominant substitution mechanisms are $Fe^{3+} \leftrightarrow V^{3+}$, $Ga^{3+} \leftrightarrow V^{3+}$, $Ti^{4+} \leftrightarrow V^{4+}$ and $2Ti^{4+} \leftrightarrow V^{3+} + Sb^{5+}$. Moreover, some of the Sb^{5+} can be replaced with Nb^{5+}.

Replacement of V by Fe and Ga gives a catalyst that compared to the $\approx SbVO_4$ base composition is considerably less active per surface area unit and more selective to acrylonitrile formation at comparable propane conversion. Substitution of V with Ti causes similar effects, although for comparable substitution levels, the activity decrease is more moderate. Replacement of Sb with Nb causes minor decrease of the activity, improved selectivity to propene and decreased selectivity to acrylonitrile.

A comparison of the catalytic data for the substituted catalysts with those of the unsubstituted $\approx SbVO_4$ clearly indicates that V-sites are the propane activating sites, whereas Sb-sites are the nitrogen inserting sites. Moreover, the results can be rationalised in terms of the site isolation theory [32,33] in that a acrylonitrile selective catalyst should have the V-centers structurally isolated and surrounded by Sb.

Acknowledgement

The Swedish Research Council is acknowledged for financial support.

References

[1] F. Cavani, F. Trifirò, Catal. Today 36 (1997) 431–439.
[2] R.K. Grasselli, M.A. Tenhover, in: G. Ertl, H. Knözinger, F. Schüth, J. Weitkamp (Eds.), Handbook of Heterogeneous Catalysis, vol. 8, second ed., Wiley-VCH, Weinheim, 2008 (Chapter 14.11.9).
[3] R.K. Grasselli, Catal. Today 49 (1999) 141–153.
[4] G. Centi, R.K. Grasselli, F. Trifirò, Catal. Today 13 (1992) 661–666.
[5] T. Ushikubo, K. Oshima, A. Kayo, T. Umezawa, K. Kiyono, I. Sawaki, European Patent 529 853 (1992), to the Mitsubishi Chemical Corporation, Tokyo, Japan.
[6] S. Komada, H. Hinago, M. Kaneta, M. Watanabe, European Patent 895 809 (1998), to Asahi Kasei Kogyo Kabushiki Kaisha, Osaka, Japan.
[7] A.T. Guttmann, R.K. Grasselli, J.F. Brazdil, U.S. Patent 4 746 641 (1988), to the Standard Oil Company, Ohios.
[8] G. Centi, R.K. Grasselli, E. Patané, F. Trifirò, Stud. Surf. Sci. Catal. 55 (1990) 515–526.
[9] J. Nilsson, A.R. Landa-Cánovas, S. Hansen, A. Andersson, J. Catal. 186 (1999) 442–457.
[10] A. Landa-Cánovas, J. Nilsson, S. Hansen, K. Ståhl, A. Andersson, J. Solid State Chem. 116 (1995) 369–377.
[11] R. Nilsson, T. Lindblad, A. Andersson, J. Catal. 148 (1994) 501–513.
[12] J. Nilsson, A. Landa-Cánovas, S. Hansen, A. Andersson, Catal. Today 33 (1997) 97–108.
[13] J. Nilsson, A.R. Landa-Cánovas, S. Hansen, A. Andersson, Stud. Surf. Sci. Catal. 110 (1997) 413–422.
[14] M.O. Guerrero-Pérez, J.L.G. Fierro, M.A. Vicente, M.A. Bañares, J. Catal. 206 (2002) 339–348.
[15] M.O. Guerrero-Pérez, M.V. Martínes, J.L.G. Fierro, M.A. Bañares, Appl. Catal. A 298 (2006) 1–7.
[16] A.T. Guttmann, R.K. Grasselli, J.F. Brazdil, U.S. Patent 4 788 317 (1988), to the Standard Oil Company, Ohio.
[17] C.S. Lynch, L.C. Glaeser, J.F. Brazdil, M.A. Toft, U.S. Patent 5 094 989 (1992), to the Standard Oil Company, Ohio.
[18] S. Albonetti, G. Blanchard, P. Burattin, F. Cavani, F. Tifirò, U.S. Patent 5 686 381 (1997), to Rhone-Poulenc Chimie, France.
[19] S. Albonetti, G. Blanchard, P. Burattin, F. Cavani, F. Tifirò, WO Patent 97/12839 (1997), to Rhone-Poulenc Fiber and Resin Intermediates, France.
[20] H. Roussel, B. Mehlomakulu, F. Belhadj, E. van Steen, J.M.M. Millet, J. Catal. 205 (2002) 97–106.
[21] N. Ballarini, F. Cavani, C. Giunchi, S. Masetti, F. Trifirò, D. Ghisletti, U. Cornaro, R. Catani, Top. Catal. 15 (2001) 111–119.
[22] N. Ballarini, F. Cavani, M. Cimini, F. Trifirò, R. Catani, U. Cornaro, D. Ghisletti, Appl. Catal. A 251 (2003) 49–59.
[23] M. Cimini, J.M.M. Millet, N. Ballarini, F. Cavani, C. Ciardelli, C. Ferrari, Catal. Today 91–92 (2004) 259–264.
[24] N. Ballarini, F. Cavani, M. Cimini, F. Trifirò, J.M.M. Millet, U. Cornaro, R. Catani, J. Catal. 241 (2006) 255–267.
[25] E. Arcozzi, N. Ballarini, F. Cavani, M. Cimini, C. Lucarelli, F. Trifirò, P. Delichere, J.M.M. Millet, P. Marion, Catal. Today 138 (2008) 97–103.
[26] N. Ballarini, F. Cavani, S. Di Memmo, F. Zappoli, P. Marion, Catal. Today 141 (2009) 264–270.
[27] M.O. Guerrero-Pérez, J.L.G. Fierro, M.A. Bañares, Catal. Today 78 (2003) 387–396.
[28] M.O. Guerrero-Pérez, J.L.G. Fierro, M.A. Bañares, Catal. Today 118 (2006) 366–372.
[29] M.O. Guerrero-Pérez, J.L.G. Fierro, M.A. Vicente, M.A. Bañares, Chem. Mater. 19 (2007) 6621–6628.
[30] J. Nilsson, A.R. Landa-Cánovas, S. Hansen, A. Andersson, J. Catal. 160 (1996) 244–260.
[31] A. Wickman, L.R. Wallenberg, A. Andersson, J. Catal. 194 (2000) 153–166.
[32] J.L. Callahan, R.K. Grasselli, AIChE J. 9 (1963) 755–760.
[33] R.K. Grasselli, J.D. Burrington, in: D.D. Eley, H. Pines, P.B. Weisz (Eds.), Advances in Catalysis, vol. 30, Academic Press, New York, 1981, pp. 133–163.
[34] T. Birchall, A.W. Sleight, Inorg. Chem. 15 (1976) 868–870.
[35] F.J. Berry, M.E. Brett, W.R.J. Patterson, Chem. Soc. Dalton Trans. (1983) 9–12.
[36] G. Aylward, T. Findlay, SI Chemical Data, fourth ed., Wiley, Brisbane, 1998.
[37] M.A. Toft, J.F. Brazdil, L.C. Glaeser, L. U.S. Patent 4 879 264 (1989), to the Standard Oil Company, Ohio.
[38] S. Hansen, K. Ståhl, R. Nilsson, A. Andersson, J. Solid State Chem. 102 (1993) 340–348.
[39] JCPDS International Centre for Diffraction Data, Powder Diffraction File, Swarthmore, PA, 1991.
[40] M.O. Guerrero-Pérez, M.A. Bañares, Catal. Today 96 (2004) 265–272.
[41] M.O. Guerrero-Pérez, M.A. Bañares, J. Phys. Chem. C 111 (2007) 1315–1322.
[42] C. Rocchiccioli-Deltcheff, T. Dupuis, R. Franck, M. Harmelin, C. Wadier, C. R. Acad. Sci. Paris Sect. B 270 (1970) 541–544.
[43] E. Husson, Y. Repelin, H. Brusset, A. Cerez, Spectrochim. Acta Sect. A 35 (1979) 1177–1187.
[44] R. Nilsson, T. Lindblad, A. Andersson, C. Song, S. Hansen, Stud. Surf. Sci. Catal. 82 (1994) 293–303.
[45] L. Abello, E. Husson, Y. Repelin, G. Lucazeau, Spectrochim. Acta Sect. A 39 (1983) 641–651.
[46] C.A. Cody, L. DiCarlo, R.K. Darlington, Inorg. Chem. 18 (1979) 1572–1576.
[47] A. Andersson, S. Hansen, A. Wickman, Top. Catal. 15 (2001) 103–110.
[48] R. Catani, G. Centi, F. Trifirò, R.K. Grasselli, Ind. Eng. Chem. Res. 31 (1992) 107–119.
[49] R.G. Teller, J.F. Brazdil, R.K. Grasselli, W. Yelon, J. Chem. Soc. Faraday Trans. 1 81 (1985) 1693–1704.
[50] F.J. Berry, J.G. Holden, M.H. Loretto, J. Chem. Soc. Faraday Trans. 1 83 (1987) 615–626.
[51] K. Brandt, Ark. Kemi. 17A (1943) No 15.
[52] S.Yu. Burylin, Z.G. Osipova, V.D. Sokolovskii, I.P. Olenkova, A.V. Kalinkin, A.V. Pashis, Kinet. Katal. 30 (1989) 494–496.
[53] W. Rüdorff, J.Z. Märklin, Z. Anorg. Allg. Chem. 334 (1964) 142–149.
[54] H. Oppermann, F. von Woedtke, T. Reich, M.A. Denecke, H. Nitsche, M. Doerr, Fresenius J. Anal. Chem. 363 (1999) 202–205.
[55] G. Centi, F. Trifirò, Catal. Rev. Sci. Eng. 28 (1986) 165–184.
[56] D.L. Nguyen, Y.B. Taarit, J.M.M. Millet, Catal. Lett. 90 (2003) 65–70.
[57] J.N. Michaels, D.L. Stern, R.K. Grasselli, Catal. Lett. 42 (1996) 139–148.
[58] J.D. Burrington, C.T. Kartisek, R.K. Grasselli, J. Catal. 87 (1984) 363–380.
[59] G. Centi, D. Pesheva, F. Trifirò, Appl. Catal. 33 (1987) 343–359.
[60] M. Bowker, C.R. Bicknell, P. Kerwin, Appl. Catal. A 136 (1996) 205–229.
[61] V. Fattore, Z.A. Fuhrman, G. Manara, B. Notari, J. Catal. 37 (1975) 223–231.
[62] I. Aso, S. Furukawa, N. Yamazoe, T. Seiyama, J. Catal. 64 (1980) 29–37.
[63] M. Carbucicchio, G. Centi, F. Trifirò, J. Catal. 91 (1985) 85–92.